



## Pressure alters electronic orbital overlap in hydrogen bonds

Hua Li<sup>a</sup>, Hiroaki Yamada<sup>b</sup>, Kazuyuki Akasaka<sup>a,b,\*</sup> & Angela M. Gronenborn<sup>c,\*</sup>

<sup>a</sup>Graduate School of Science and Technology and <sup>b</sup>Faculty of Science, Kobe University; <sup>c</sup>Laboratory of Chemical Physics, National Institute of Diabetes and Digestive and Kidney Diseases, National Institutes of Health, Bethesda, MD 20892, U.S.A.

Received 4 July 2000; Accepted 14 August 2000

**Key words:** GB1, H-bonds, J coupling, pressure, proteins

### Abstract

Pressure-induced changes in  ${}^3\text{h}J_{\text{NC}'}$  scalar couplings through hydrogen bonds were investigated in the immunoglobulin binding domain of streptococcal protein G.  ${}^1\text{H}$ ,  ${}^{15}\text{N}$  and  ${}^{13}\text{C}$  triple-resonance NMR spectroscopy coupled with the on-line high pressure cell technique was used to monitor  ${}^3\text{h}J_{\text{NC}'}$  scalar couplings at 30 and 2000 bar in uniformly labeled  ${}^{15}\text{N}$  and  ${}^{13}\text{C}$  protein isotopes. Both increased and decreased  ${}^3\text{h}J_{\text{NC}'}$  scalar couplings were observed at high pressure. No correlation with secondary structure was apparent. The difference in coupling constants as well as pressure-induced chemical shift data suggests a compaction of the helix ends and an increase of the helix pitch at its center in response to pressure. Our data provides the first direct evidence that the electronic orbital overlap in protein backbone hydrogen bonds is altered by pressure.

**Abbreviations:** H bond, hydrogen bond; ZQ/DQ, Zero-Quantum/Double-Quantum; DSS, 2,2-dimethyl-2-silapentane-5-sulfonate; CT-HNCO, constant time - HNCO; HSQC, Heteronuclear Single Quantum Correlation.

### Introduction

Hydrogen bonds (H bonds) are of key importance for stabilizing biomolecular structure and for modulating the substrate binding specificity and reaction rate of virtually any enzymatic reaction. The importance of hydrogen bonds in biomolecules was already emphasized 50 years ago in the proposal of the secondary structure models of proteins,  $\alpha$ -helix and  $\beta$ -sheet, and the Watson–Crick base-pairing in DNA (Hadzi and Tompson, 1959; Pimentel and McClellan, 1960). These proposed models stimulated chemists' interest into the nature of these hydrogen bonds. However, the existence of hydrogen bonds is usually inferred, rather than directly observed by experiments. In three-dimensional models of macromolecules, solved by X-ray crystallography or NMR, the presence of H

bonds is primarily deduced based on the spatial proximity and relative arrangement of the atoms involved. In NMR derived models, a variety of spectroscopic parameters are also employed for characterizing these pivotal interactions. These include empirical effects of hydrogen bonding on isotropic chemical shifts (Wagner et al., 1983) and chemical shift anisotropy (Tjandra and Bax, 1997), on the quadrupole coupling of the  ${}^2\text{H}$  nucleus involved in H bonds (LiWang and Bax, 1997) and on sequential  ${}^1J_{\text{NC}'}$  coupling constants (Juranic et al., 1995). In addition, H-bonding affects the exchange of labile hydrogens with solvent hydrogen (Wagner, 1984) and  ${}^1\text{H}/{}^2\text{H}$  fractionation (Lin et al., 1998).

Recently, Dingley and Grzesiek (1998) were the first to demonstrate the presence of surprisingly large  $J$  couplings (6–7 Hz) between the H bond-donating and -accepting  ${}^{15}\text{N}$  nuclei in a Watson–Crick base pair in double-stranded RNA. This finding was confirmed by Pervushin et al. (1998), who also discovered the presence of smaller (2–4 Hz)  $J$  couplings between

\*To whom correspondence should be addressed. E-mail: gronenborn@nih.gov

The U.S. Government's right to retain a non-exclusive, royalty free licence in and to any copyright is acknowledged.

the imino hydrogen itself and the H bond accepting  $^{15}\text{N}$  nucleus. Later, the presence of  $^3\text{h}J_{\text{NC}'}$  interactions across backbone-backbone H bonds was also reported in small proteins such as ubiquitin (Cordier and Grzesiek, 1999; Cornilescu et al., 1999a) and the immunoglobulin binding domain of streptococcal protein G (Cornilescu et al., 1999b) and in a protein as large as 30 kDa (Wang et al., 1999). Furthermore, a good correlation between  $^3\text{h}J_{\text{NC}'}$  couplings and H bond length was found in protein G, and the sign of  $^3\text{h}J_{\text{NC}'}$  was also determined from a ZQ/DQ experiment. These couplings confirm the overlap of the electronic orbitals of the atoms involved, and most importantly, identify unambiguously the pairs of atoms involved in a given H bond. Interestingly, a recent Compton X-ray scattering study of hexagonal ice also found evidence for a partial covalent character of H bonds (Isaacs et al., 1999).

Since pressure is a variable that directly acts on inter atomic distances, pressure effects on H-bonding interactions have been studied by NMR for a long time. In simple protic liquids such as water and methanol, high pressure induces low-field shifts of the H bonded protons (Linowski et al., 1976a, b). These shifts were attributed to the compression of the liquids and shortening of the H bonds. Recently, an on-line high pressure cell NMR technique was developed by our group (Yamada, 1974; Akasaka et al., 1997). It is based on fitting a high pressure cell into a standard commercial NMR probe. Initial studies on several proteins revealed that almost all the amide protons of proteins experienced a downfield shift at high pressure (Inoue et al., 1998; Li et al., 1998). Based upon an empirical distance-shift relationship (Wagner et al., 1983), intramolecular H bonds between amide protons and carbonyl oxygens were estimated to be shortened by  $\sim 1\%$  on average at 2000 bar. The effect of pressure on amide  $^{15}\text{N}$  chemical shifts was studied by  $^1\text{H}$ - $^{15}\text{N}$  heteronuclear correlation spectroscopy between 1 and 2000 bar (Akasaka et al., 1998; Kalbitzer et al., 2000). Most  $^{15}\text{N}$  signals were low field shifted linearly and reversibly, but non-uniformly, with pressure, suggesting a variation of site-specific changes in  $\phi$ ,  $\psi$  angles, in addition to a decrease in H bonding distances. Our current methodology also allows us to monitor pressure effects on rapid (Sareth et al., 2000) and slow (Li et al., 1999) motions of proteins. We therefore decided to directly investigate the change in electronic overlap in H bonds between nitrogen and carbonyl carbon nuclei in a protein by monitoring the effects of pressure on the  $^3\text{h}J_{\text{NC}'}$  couplings.

As a target protein, we selected the immunoglobulin (IgG) binding domain of streptococcal protein G (GB1) in which  $^3\text{h}J_{\text{NC}'}$  scalar couplings through hydrogen bonds have been measured for 34 H bond pairs (Cornilescu et al., 1999). GB1 is a small domain of only 56 residues and exhibits extreme stability towards both heat and urea denaturation, despite the absence of any disulfide bridges (Gronenborn et al., 1991; Gronenborn and Clore, 1993). The three-dimensional solution structure of GB1 was solved by NMR (Gronenborn et al., 1991; Gronenborn and Clore, 1993) and X-ray crystallography (Gallagher et al., 1994). In addition, numerous other biophysical characterizations have been carried out (Achari et al., 1992; Clore and Gronenborn, 1992; Gronenborn and Clore, 1993; Barchi et al., 1994). All structures reveal a highly compact globular protein with a tightly packed hydrophobic core in which 95% of the residues participate in regular secondary structure. The latter comprises a four-stranded  $\beta$ -sheet consisting of two antiparallel  $\beta$ -hairpins connected by an  $\alpha$ -helix.

## Methods

### *High pressure NMR apparatus*

The on-line high pressure cell method (Yamada, 1974) was interfaced with a Bruker DMX-750 NMR spectrometer operating at 750.13 MHz for  $^1\text{H}$  and 76.01 MHz for  $^{15}\text{N}$ . The protein solution in a quartz tube (inner diameter of 1 mm, outer diameter of 3 mm, protected by a Teflon jacket) is connected through a frictionless teflon piston to kerosene in a long stainless steel tubing, connected to a remote hand pump. One can set the pressure of the sample solution at any pressure between 1 and 2000 bar (measured with a Heise Bourdon gauge). The sample was positioned in the NMR probe, which is a commercial 5 mm  $^1\text{H}$ -detection inverse probe with an  $x$ ,  $y$ ,  $z$ -field gradient coil.

### *NMR measurements*

NMR measurements at various pressures were carried out at 25 °C.  $^{13}\text{C}$ ,  $^{15}\text{N}$ -labeled protein G was dissolved into 100 mM MES buffer in  $\text{H}_2\text{O}/\text{D}_2\text{O}$  (90:10, v/v), to obtain a concentration of 10 mM at pH 5.6. Dioxan and DSS were added as internal chemical shift references. MES buffer was used because of its small  $\Delta V$  value so that the pH changes in the NMR sample solution induced by pressure could be ignored (Good

and Izawa, 1972).  ${}^3\text{h}J_{\text{NC}}$  couplings were measured with a 2D CT-HNCO experiment (Cornilescu et al., 1999b). The scheme was executed three times at two pressures, 30 and 2000 bar, respectively: (A) with the dephasing time,  $2T$ , tuned to  $1/(2^1J_{\text{NC}'})$ , (B) with  $2T = 3/(2^1J_{\text{NC}'})$ , (C) with  $2T = 4/(2^1J_{\text{NC}'})$ . A pressure of 30 bar instead of 1 bar was purely chosen due to technical reasons. All spectra were recorded as  $128^* \times 1024^*$  data matrixes, with 64 scans per complex  $t_1$  increment for (A) measurement ( $\sim 7$  h), 64 scans for (B) ( $\sim 8$  h), and 1024 scans for (C) ( $\sim 5$  d 14 h).

In addition to the  ${}^3\text{h}J_{\text{NC}'}$  measurements,  ${}^1\text{H}$ ,  ${}^{15}\text{N}$ -HSQC (Bodenhausen and Rubin, 1980) and 2D CT-HNCO (with  $2T = 1/(2^1J_{\text{NC}'})$ ) experiments were carried out at six pressures of 30, 400, 800, 1200, 1600, 2000 bar, in order to follow each cross peak gradually with pressure. In this manner, unambiguous assignments at 2000 bar are achieved. This also allows the determination of the pressure dependence of chemical shifts.  ${}^{15}\text{N}$  and  ${}^{13}\text{C}'$  chemical shifts are referenced indirectly as described by Wishart et al. (1995).

Data processing was carried out using the program NMRPipe (Delaglio et al., 1995) and xwinmr.

## Results and discussion

### *Pressure-induced changes in ${}^1\text{H}^{\text{N}}$ , ${}^{15}\text{N}$ and ${}^{13}\text{C}'$ chemical shifts*

${}^1\text{H}$ ,  ${}^{15}\text{N}$ -HSQC and 2D CT-HNCO experiments were recorded for six pressures of 30, 400, 800, 1200, 1600, 2000 bar. The observed chemical shift changes for all amide protons are plotted in Figure 1. Likewise,  ${}^{15}\text{N}$  and  ${}^{13}\text{C}'$  shifts also exhibit almost linear, reversible but non-uniform changes over this pressure range. The continuous and linear chemical shift changes with pressure are a clear indication that the protein remains fully folded within the native ensemble similarly to the case of BPTI (Li et al., 1998; Akasaka et al., 1999; Sareth et al., 2000). Figure 2 summarizes the chemical shift changes for  ${}^1\text{H}^{\text{N}}$ ,  ${}^{15}\text{N}$  and  ${}^{13}\text{C}'$ . For each residue the slope of the change is plotted in histogram fashion. For the amide protons and carbonyl carbons, those involved in backbone H-bonding are shown in black while others are shown in grey. As can be appreciated, most resonances experience downfield shifts, although no uniform behavior is observed.

The chemical shift of  ${}^1\text{H}^{\text{N}}$  and  ${}^{13}\text{C}'$  is a sensitive measure of the H bonding state. The present study reveals that the average chemical shift change for a  ${}^1\text{H}^{\text{N}}$

involved in a H bond is 0.039 ppm/2 kbar, whereas a  ${}^1\text{H}^{\text{N}}$  not involved in a H bond experiences an average shift of 0.069 ppm/2 kbar. For the carbonyl carbon, the average chemical shift for a  ${}^{13}\text{C}'$  involved in a H bond is 0.056 ppm/2 kbar, and for one not involved in a H bond it is 0.023 ppm/2 kbar. Unfortunately, these average values are not very helpful for predicting or explaining local effects and a more detailed discussion is given below.

The size of the pressure-induced chemical shifts of  ${}^{15}\text{N}$  was previously suggested to correlate with the flexibility of the backbone (Akasaka et al., 1999; Kalbitzer et al., 2000). The average value of the pressure-induced chemical shift changes in  ${}^{15}\text{N}$  for the different secondary structural elements of protein G is  $0.320 \pm 0.390$  ppm/2 kbar for  $\beta 1$ ,  $0.697 \pm 0.470$  ppm/2 kbar for  $\beta 2$ ,  $0.189 \pm 0.350$  ppm/2 kbar for  $\beta 3$ ,  $0.313 \pm 0.311$  ppm/2 kbar for  $\beta 4$ , and  $0.422 \pm 0.347$  ppm/2 kbar for the helix. It is interesting to note that the largest average value is observed for  $\beta$ -strand 2 and indeed the largest changes for any residues are observed for residues 13 and 14 in  $\beta 2$ . It is known from the  ${}^{15}\text{N}$  relaxation study on protein G (Achari et al., 1992) that the two central strands  $\beta 1$  and  $\beta 4$  are essentially rigid, while  $\beta 2$  and  $\beta 3$ , and in particular  $\beta$ -strand 2, are more mobile than the inner two strands. Moreover,  $\beta$ -strand 2 not only has lower order parameters than the other strands but several residues experience slower motions on the nanosecond to millisecond time scale. The fact that the largest pressure-induced shifts are observed for residues in  $\beta 2$  and in a loop connecting the helix to  $\beta 3$  is consistent with the notion that the size of the pressure-induced  ${}^{15}\text{N}$  shifts correlates with the flexibility of the backbone (Akasaka et al., 1999; Kalbitzer et al., 2000).

### *Pressure-induced changes in transverse relaxation times ( $T_2$ )*

In a 2D CT-HNCO experiment, the signal intensity observed for a correlation between  ${}^{15}\text{N}$  and  ${}^{13}\text{C}'$  with a coupling  $J_{\text{NC}'}$  is proportional to  $\exp(-4T/T_2)\sin^2(2\pi J_{\text{NC}'}) \prod_k \cos^2(2\pi J_{\text{NK}})$ , with the product extending over all other carbonyl/carboxyl carbons coupled with coupling constants  $J_{\text{NK}}$ , to the  ${}^{15}\text{N}$  of interest.  $T_2$  is the  ${}^{15}\text{N}$  transverse relaxation time. A good estimate for  $T_2$  can be obtained from the ratio of two experiments A and B recorded with different dephasing times (cf. Methods section). Figure 3 illustrates the transverse relaxation time ( $T_2$ ) of  ${}^{15}\text{N}$  at 30 bar and 2000 bar (lower part), and the

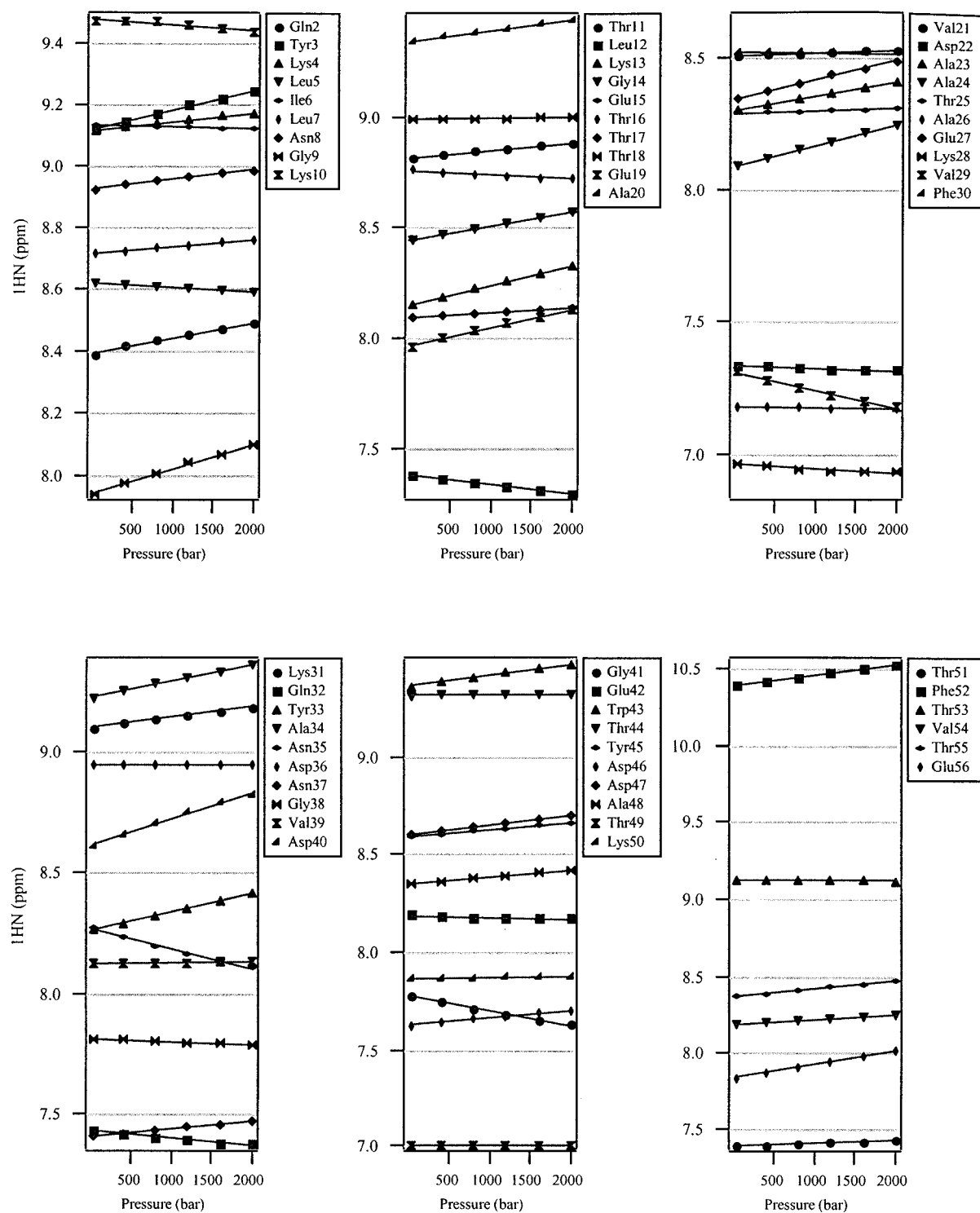


Figure 1. Chemical shifts of the amide protons ( $^1\text{H}^{\text{N}}$ ) in GB1 for six different pressures. The first two panels comprise residues located in strand  $\beta 1$  and  $\beta 2$ , the second and third depict helical residues and panels five and six show those located in strand  $\beta 3$  and  $\beta 4$ .

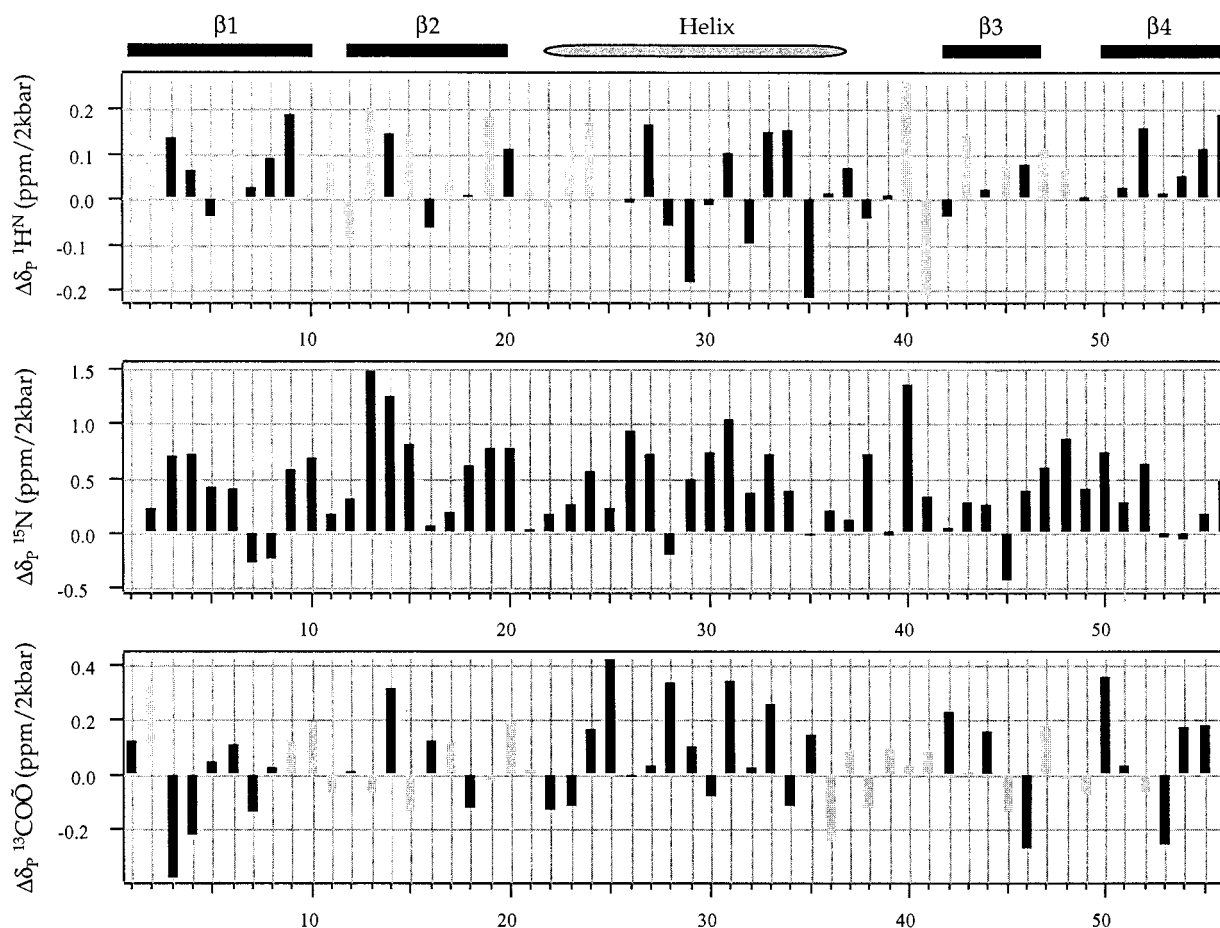


Figure 2. Chemical shift differences for amide protons ( $^1\text{H}^{\text{N}}$ ), amide nitrogens ( $^{15}\text{N}$ ) and carbonyl carbons ( $^{13}\text{C}'$ ) plotted against the residue number. They are expressed as slopes obtained from linear curve fitting. For  $^1\text{H}^{\text{N}}$  and  $^{13}\text{C}'$ , those involved in backbone H bonds are shown by dark, solid columns, others are shown by light dotted columns. The secondary structures are shown at the top.

pressure-induced changes of the transverse relaxation rate ( $\Delta R_2$ ) (upper part).  $T_2$  values for residues Tyr 3, Lys 4, Gly 38, Glu 56 at 30 bar and Ile 6, Thr 53 at 2000 bar could not be determined because of signal overlap. As can be easily appreciated, the pattern of  $T_2$  for each residue at both pressures is very similar, with  $\Delta R_2$  ranging from  $0.47 \text{ s}^{-1}$  to  $-0.84 \text{ s}^{-1}$ . Thus, it appears that  $T_2$  relaxation rates are insensitive to pressure for the pressure range up to 2 kbar. This result is consistent with the observed linear pressure dependence of chemical shifts, and suggests that the protein remains in the same native ensemble at 1 bar with a small shift of population, similar to BPTI (Sareth et al., 2000).

#### Pressure-induced changes in $^3\text{h}J_{\text{NC}'}$

Based on a good estimate of  $T_2$ , the magnitude of the small coupling between N and  $k$  can be derived from the relationship

$$\sin^2(2\pi J_{\text{Nk}}T) = I^{\text{C}} \exp(1/{}^1J_{\text{NC}'T_2})/I^{\text{B}} \quad (\text{a})$$

where  $I^{\text{C}}$  is the intensity of the (weak) correlation between  $^{15}\text{N}$  and  $k$ , and  $I^{\text{B}}$  is the intensity of the one-bond N-C' correlation. The former is obtained with a dephasing time  $2T = 3/(2{}^1J_{\text{NC}'})$  and the latter with  $2T = 4/(2{}^1J_{\text{NC}'})$ .

Values of through H bond  $^3\text{h}J_{\text{NC}'}$  were obtained for protein G at 30 and 2000 bar, respectively. Due to the small sample volume ( $\sim 20 \mu\text{l}$ ) and the small value of  $^3\text{h}J_{\text{NC}'}$ , the signal to noise ratio in the present 2D CT-HNCO experiment is quite limited. As a result, only eleven  $^3\text{h}J_{\text{NC}'}$  were obtained with sufficient accuracy

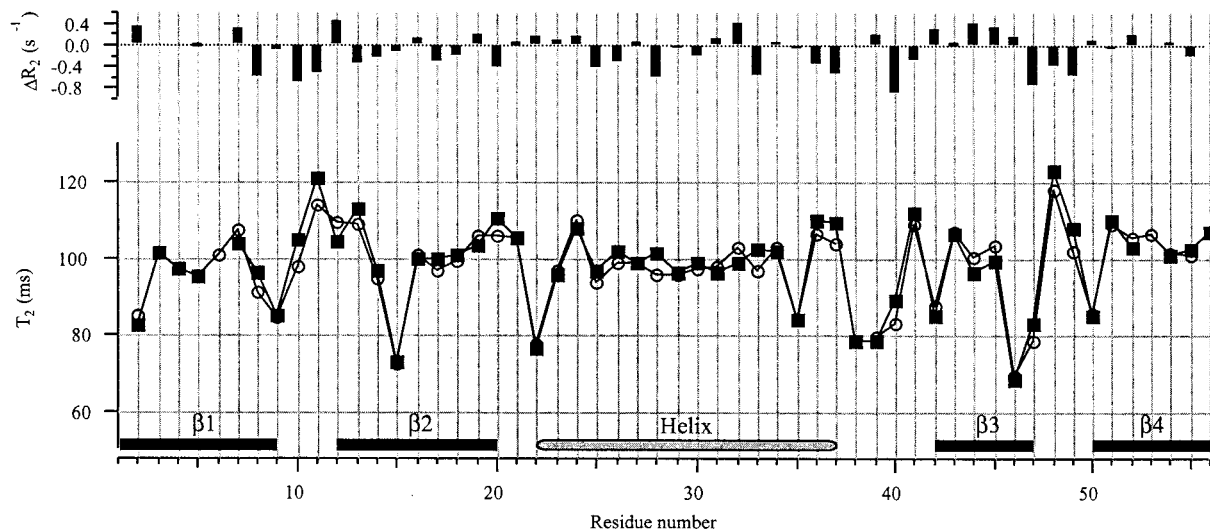


Figure 3. Pressure dependence of the transverse relaxation time of  $^{15}\text{N}$  ( $T_2$ ). (Upper) Pressure-induced changes in the transverse relaxation rates of  $^{15}\text{N}$  ( $\Delta R_2$ ) plotted against the residue number, where  $\Delta R_2 = 1/T_2$  (2000 bar)  $- 1/T_2$  (30 bar). (Lower) Transverse relaxation times of  $^{15}\text{N}$  ( $T_2$ ) at 30 bar (open circles connected by dotted line) and at 2000 bar (solid squares connected by solid line) plotted against the residue number.

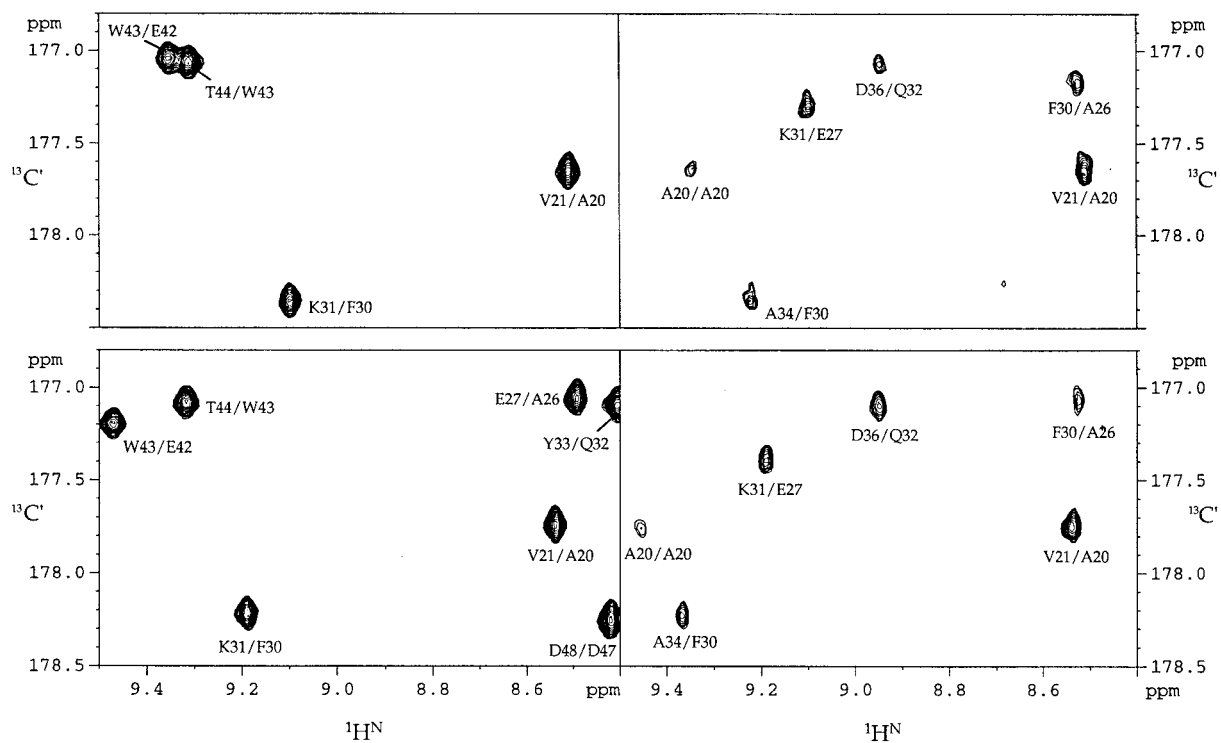


Figure 4. Representative regions of 2D CT-HNCO spectra obtained with different dephasing time; 100 ms (left) and 132 ms (right), at 30 bar (upper panel) and 2000 bar (lower panel). Each cross peak is marked by the residue number for the amide proton and the carbonyl carbon involved.

for both pressures, while two  $^3\text{h}J_{\text{NC}'}$  (Tyr 3 and Thr 53) could only be obtained at either 30 bar or 2000 bar due to signal overlap. Compared with previous results (Cornilescu et al., 1999), only those  $^3\text{h}J_{\text{NC}'}$  which are larger than 0.50 Hz could be measured reliably in the high pressure cell. Two regions of the 2D CT-HNCO spectra with two different dephasing times of 100 ms and 132 ms at 30 and 2000 bar, respectively are plotted in Figure 4. The  $^3\text{h}J_{\text{NC}'}$  values (absolute values) calculated from the experimental data at the two pressures are listed in Table 1. The present values are very close to those reported previously in a conventional set up (Cornilescu et al., 1999). Small differences were found for the H bond pairs, Leu7-Gly14, Ala34-Phe30 and Asp36-Gln32. Pressure-induced changes in  $^3\text{h}J_{\text{NC}'}$  range from +0.08 Hz to -0.12 Hz. Using the empirical correlation  $R_{\text{NO}} = 2.75 - 0.25 \ln(-^3\text{h}J_{\text{NC}'}) \pm 0.06 \text{ \AA}$  (Cornilescu et al., 1999) these values correspond to changes in the H bond distance ranging from +0.045 \AA to -0.037 \AA.

It is interesting that not only increased (H bond pairs of Ala20-Met1, Glu27-Ala23, Ala34-Phe30, Asp36-Gln32 and Phe52-Lys4), but also decreased (H bond pairs of Leu7-Gly14, Phe30-Ala26, Lys31-Glu27 and Thr44-Thr53)  $^3\text{h}J_{\text{NC}'}$  couplings were detected at high pressure. In addition, for some H bond pairs (Leu5-Thr16 and Asn8-Val54) the couplings remained unchanged. No grouping according to secondary structure elements was observed. Figure 5 (left) illustrates all measured  $^3\text{h}J_{\text{NC}'}$  couplings on the secondary structure diagram of GB1. Increased  $^3\text{h}J_{\text{NC}'}$  couplings induced by pressure are shown as red arrows, decreased  $^3\text{h}J_{\text{NC}'}$  as blue arrows, and  $^3\text{h}J_{\text{NC}'}$  exhibiting no change are colored yellow. The positions of the corresponding amides and carbonyls within the three dimensional structure of GB1 are color coded using the identical color scheme in a stereo diagram at the bottom of Figure 5. Interestingly, we find that the increased  $^3\text{h}J_{\text{NC}'}$  couplings are mainly located at peripheral regions of secondary structure such as  $\beta$  strands (Ala20-Met1 and Phe52-Lys4) and the helix ends (Glu27-Ala23, Ala34-Phe30, and Asp36-Gln32). Decreased  $^3\text{h}J_{\text{NC}'}$  couplings are observed for H bonds at the center of the protein, both in the helix (Phe30-Ala26 and Lys31-Glu27) as well as in the middle of the two antiparallel hairpins (Leu7-Gly14 and Thr44-Thr53). It thus appears that buried, rigid regions and exposed, flexible regions respond differently to pressure. It was deduced from a comparison of the X-ray structures of lysozyme at 1 bar and 1 kbar that no simple rules exist for how a protein structure responds

to pressure. Very little changes in atomic coordinates were observed for  $\beta$ -sheet regions, some deformation was observed for some helices and one loop region appeared to expand (Kundrot and Richards, 1987). Unfortunately, large changes in B factors, up and down in value, were observed for individual atoms which could not be rationalized. Our results report on H-bonding within the protein structure. An increase in the  $^3\text{h}J_{\text{NC}'}$  coupling could arise from a decrease in the distance or possibly more favorable N-H $\cdots$ O and H $\cdots$ O=C angles. Inspection of the highest resolution X-ray structure for an immunoglobulin binding domain of protein G (Derrick and Wigley, 1994) reveals that there is essentially no difference in angle for the H-bonding pairs Phe30-Ala26 and Lys31-Glu27, whose values are reduced, and those of Glu27-Ala23, Ala34-Phe30, and Asp36-Gln32, whose values are increased by pressure whereas the separation  $R_{\text{NO}}$  between the amide nitrogen and the oxygen atom varies by more than 0.2 \AA. Thus, it seems more likely that a difference in atomic separation is the primary cause for the increased or decreased coupling. Since no significant cavities or voids are found in the GB1 structure the compressibility of this protein has to be relatively small. Maybe the small decreases in coupling observed for the central part of the protein are due to small distortions of the optimal H-bond parameters, such as an increase in distance or a small change in angle.

The pressure-induced changes in  $^3\text{h}J_{\text{NC}'}$  couplings are compared to changes in chemical shifts of the amide protons. In general, downfield (or upfield) shifts of amide protons induced by pressure imply H bond shortening (or elongation) (Li et al., 1998; Akasaka et al., 1999). In the present case, the large downfield shifts observed for amide protons of Ala20, Glu27, Ala34, and Phe52 are consistent with the pressure-induced increases in  $^3\text{h}J_{\text{NC}'}$  couplings between H bond pairs of Ala20-Met1, Glu27-Ala23, Ala34-Phe30, and Phe52-Lys4. Figure 6 shows a stereo view of the GB1 structure on which the pressure induced amide shift changes are mapped. Amide protons are color-coded into four groups according to different ranges of the pressure-induced shifts ( $\Delta\delta_{\text{p}}$ ):  $\Delta\delta_{\text{p}} > 0.09$  ppm (red),  $0.03 < \Delta\delta_{\text{p}} < 0.09$  ppm (green),  $-0.03 < \Delta\delta_{\text{p}} < 0.03$  ppm (yellow), and  $\Delta\delta_{\text{p}} < -0.03$  ppm (blue). Interestingly, for the helix, high field shifts were observed for the amide protons of Lys28, Val29, Gln32, and Asn35 (Figure 6, blue), in contrast to the downfield shifts observed for most amide protons (red). These residues are located on the solvent exposed face of the helix, and based on shift considerations alone, it

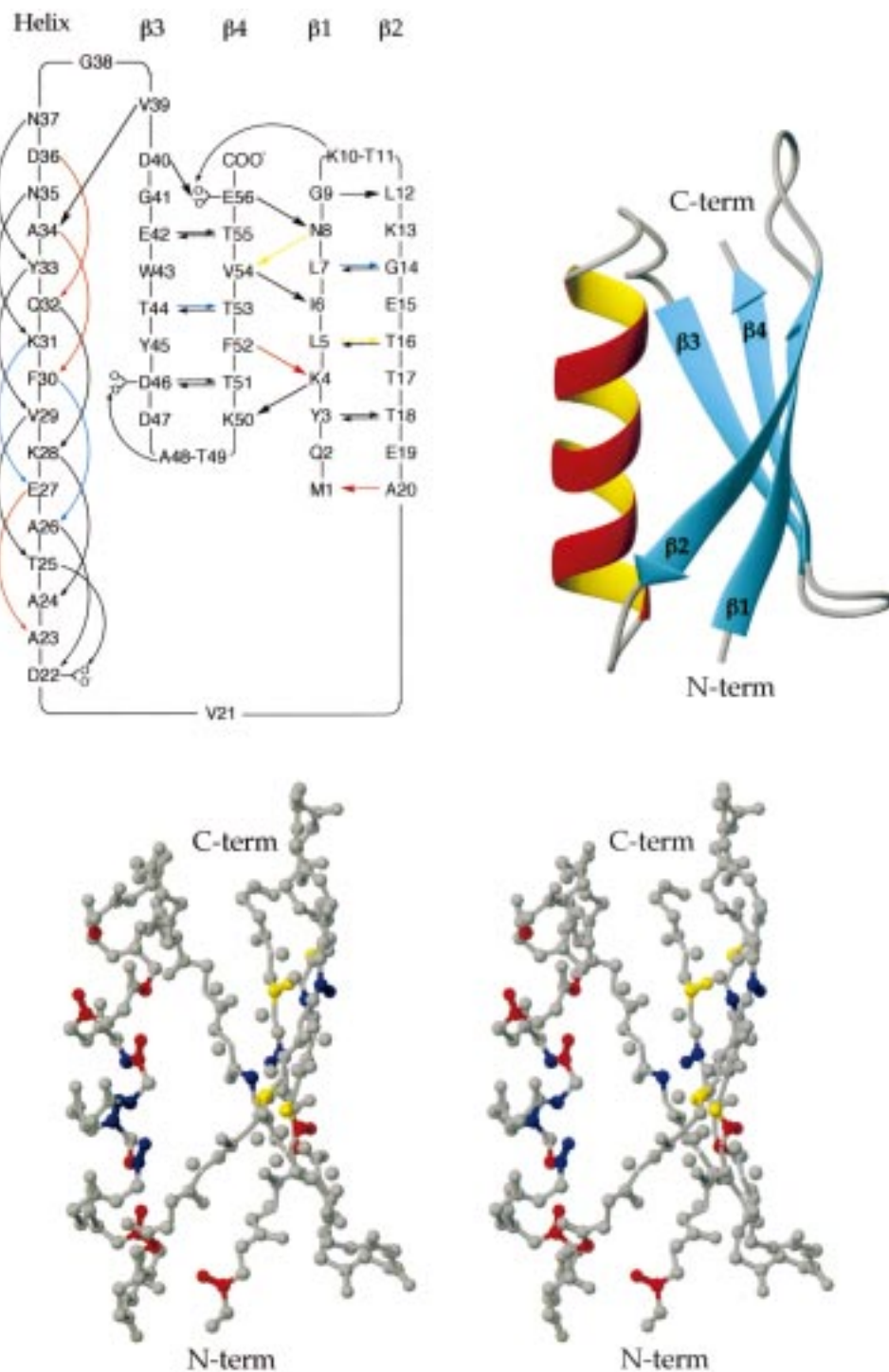


*Figure 5.* Pressure effects on the hydrogen bond network of GB1. (Top left) Schematic drawing of the secondary structure of GB1 with all the observed  $^3hJ_{NC'}$  correlations marked by arrows (Cornilescu et al., 1999b). Increased  $^3hJ_{NC'}$  couplings induced by pressure are indicated by red arrows, decreased  $^3hJ_{NC'}$  couplings are indicated by blue arrows, and  $^3hJ_{NC'}$  with no change are indicated by yellow arrows. (Top right) Ribbon diagram of the IgG-binding domain of protein G. (Bottom) Stereo view of the backbone trace of IgG-binding domain of protein G drawn in the same orientation as the ribbon diagram. For all the observed main chain  $^3hJ_{NC'}$  connections, the amide nitrogen and carbonyl groups are colored. The H bond pairs with increased  $^3hJ_{NC'}$  are colored red, those with decreased  $^3hJ_{NC'}$  are colored blue, and those unchanged yellow. Both, the ribbon diagram and the backbone trace drawing were made using the program MOLMOL (Koradi et al., 1996).

Table 1.  $^3\text{h}J_{\text{NC}'}$  couplings in protein G measured using the on-line high pressure NMR technique at 30 bar and 2000 bar, the average H bond length, secondary structure location of the H bond pairs, and the pressure-induced changes in  $^3\text{h}J_{\text{NC}'}$  couplings ( $\Delta^3\text{h}J_{\text{NC}'}$ ) and NO  $\bullet\bullet\bullet$  distances ( $\Delta R_{\text{NO}}$ )

H bond pairs		Secondary structure <sup>a</sup>	$R_{\text{NO}}^{\text{b}}$ (Å)	$^3\text{h}J_{\text{NC}'}^{\text{c}}$ (Hz)		$\Delta^3\text{h}J_{\text{NC}'}$ (Hz)	$\Delta R_{\text{NO}}^{\text{d}}$ (Å)
$^1\text{H}^{\text{N}}$	$^{13}\text{C}'$			30 bar	2000 bar		
Tyr 3	Thr 18	$\beta$	2.88	e (0.51)	0.63		
Leu 5	Thr 16	$\beta$	2.88	0.71 (0.70)	0.69	-0.02	+0.008
Leu 7	Gly 14	$\beta$	2.85	0.59 (0.68)	0.47	-0.12	+0.045
Asn 8	Val 54	$\beta$	2.87	0.73 (0.70)	0.71	-0.02	+0.008
Ala 20	Met 1	$\beta$	2.97	0.50 (0.51)	0.54	+0.04	-0.024
Glu 27	Ala 23	$\alpha$	2.90	0.50 (0.54)	0.58	+0.08	-0.037
Phe 30	Ala 26	$\alpha$	2.91	0.64 (0.64)	0.56	-0.08	+0.038
Lys 31	Glu 27	$\alpha$	2.84	0.73 (0.72)	0.68	-0.05	+0.018
Ala 34	Phe 30	$\alpha$	2.91	0.56 (0.49)	0.63	+0.07	-0.034
Asp 36	Gln 32	$\alpha$	2.82	0.52 (0.60)	0.58	+0.06	-0.020
Thr 44	Thr 53	$\beta$	2.95	0.57 (0.53)	0.52	-0.05	+0.028
Phe 52	Lys 4	$\beta$	2.80	0.75 (0.70)	0.82	+0.07	-0.022
Thr 53	Thr 44	$\beta$	2.92	0.47 (0.61)	e		

<sup>a</sup>The secondary structure type of the individually detected H bond pairs is indicated.

<sup>b</sup> $R_{\text{NO}}$  values were averaged over three crystal structures (1PGB, 1IGD and 2IGD).

<sup>c</sup>The absolute values of  $^3\text{h}J_{\text{NC}'}$  are presented without considering their sign. Previously reported values are given in parentheses.

<sup>d</sup>H bond distance changes are calculated here according to the correlation (Cornilescu et al., 1999) between  $^3\text{h}J_{\text{NC}'}$  and  $R_{\text{NO}}$ :  $^3\text{h}J_{\text{NC}'} = -59000 \exp(-4R_{\text{NO}}) \pm 0.09$  Hz.

<sup>e</sup> $^3\text{h}J_{\text{NC}'}$  values which could not be calculated precisely because of signal overlap.

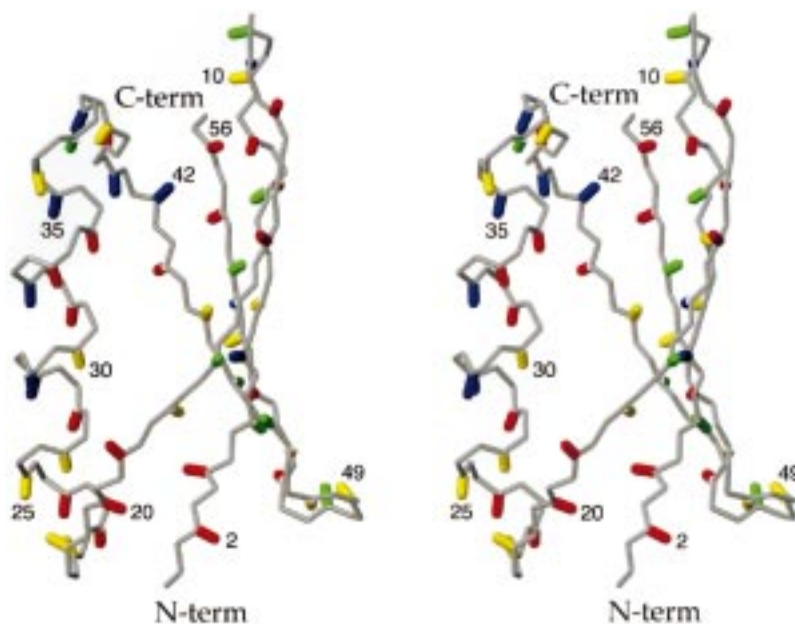


Figure 6. Pressure effects on the amide hydrogens of GB1. The NH bonds are color-coded into four groups according to different ranges of the pressure-induced shifts ( $\Delta\delta_{\text{p}}$ ) of the amide protons:  $\Delta\delta_{\text{p}} > 0.09$  ppm (red),  $0.03 < \Delta\delta_{\text{p}} < 0.09$  ppm (green),  $-0.03 < \Delta\delta_{\text{p}} < 0.03$  ppm (yellow), and  $\Delta\delta_{\text{p}} < -0.03$  ppm (blue).

appears that an increase in H-bonding distance occurs. Such high field shifts of amide protons under high pressure were also observed in a helical region in a histidine containing protein (HPr) (Kalbitzer et al., 2000). In addition to the external amides on the helix, several amide protons in the loop connecting the helix to  $\beta$ -strand 3 experience pressure induced high field shifts. This is a region of the protein which exhibits a higher degree of mobility at atmospheric pressure (Achari et al., 1992). Thus, it may well be that pressure leads to a structural rearrangement of this region resulting in a small bend in the helix towards the sheet. This would naturally elongate the H bonds on the external face of the helix.

### Concluding remarks

The present study investigated effects of pressure on hydrogen bonding in proteins. Not only increased, but also decreased  $^3\text{H}J_{\text{NC}'}$  scalar couplings were detected at high pressure. Increased  $^3\text{H}J_{\text{NC}'}$  couplings were found mainly in the loop and the peripheral region of the helix, while decreased couplings were observed at the very center of the protein. Since these couplings are directly related to the H-bond distances and electronic overlap, it seems that longer distances, i.e. a weakening of H-bonds occurs under pressure at the very center of the GB1 structure whereas stronger H-bonding occurs at the periphery. Our data demonstrate for the first time that the electronic orbital overlap within a hydrogen bond is altered by pressure.

### Acknowledgements

We are greatly indebted to the technical assistance and advice given by Dr Markus Waelchli of Bruker Japan in performing this difficult experiment. H. L. is supported by a JSPS fellowship.

### References

- Achari, A., Hale, S.P., Howard, A.J., Clore, G.M., Gronenborn, A.M., Hardman, K.D. and Whitlow, M. (1992) *Biochemistry*, **31**, 10449–10457.
- Akasaka, K., Tezuka, T. and Yamada, H. (1997) *J. Mol. Biol.*, **271**, 671–678.
- Akasaka, K., Li, H., Yamada, H., Li, R., Thoresen, T. and Woodward, C.K. (1999) *Protein Sci.*, **8**, 1946–1953.
- Barchi Jr., J.J., Grasberger, B., Gronenborn, A.M. and Clore, G.M. (1994) *Protein Sci.*, **3**, 15–21.
- Bodenhausen, G. and Rubin, D.J. (1980) *Chem. Phys. Lett.*, **69**, 185–189.
- Clore, G.M. and Gronenborn, A.M. (1992) *J. Mol. Biol.*, **223**, 853–856.
- Cordier, F. and Grzesiek, S. (1999) *J. Am. Chem. Soc.*, **121**, 1601–1602.
- Cornilescu, G., Hu, J.-S. and Bax, A. (1999a) *J. Am. Chem. Soc.*, **121**, 2949–2950.
- Cornilescu, G., Ramirez, B.E., Frank, M.K., Clore, G.M., Gronenborn, A. M. and Bax, A. (1999b) *J. Am. Chem. Soc.*, **121**, 6275–6279.
- Delaglio, F., Grzesiek, S., Vuister, G.W., Zhu, G., Pfeifer, J. and Bax, A. (1995) *J. Biomol. NMR*, **6**, 277–293.
- Derrick, J.P. and Wigley, D.B. (1994) *J. Mol. Biol.*, **243**, 906–918.
- Dingley, A.J. and Grzesiek, S. (1998) *J. Am. Chem. Soc.*, **120**, 8293–8297.
- Gallagher, T., Alexander, P., Bryan, P. and Gilliland, G.L. (1994) *Biochemistry*, **33**, 4721–4729.
- Good, N.E. and Izawa, S. (1972) *Methods Enzymol.*, **24**, 53–68.
- Gronenborn, A.M. and Clore, G.M. (1993) *Immunol. Methods*, **2**, 3–8.
- Gronenborn, A.M. and Clore, G.M. (1993) *J. Mol. Biol.*, **233**, 331–335.
- Gronenborn, A.M., Filpula, D.R., Essig, N.Z., Achari, A., Whitlow, M., Wingfield, P.T. and Clore, G.M. (1991) *Science*, **253**, 657–661.
- Hadzi, D. and Tompson, H.W. (1959) *Hydrogen Bonding*, Pergamon Press, London.
- Inoue, K., Yamada, H., Imoto, T. and Akasaka, K. (1998) *J. Biomol. NMR*, **12**, 535–541.
- Isaacs, E.D., Shukla, A., Platzmann, P.M., Barbiellini, B. and Tulk, C.A. (1999) *Phys. Rev. Lett.*, **82**, 600–603.
- Juranic, N., Ilich, P.K. and Macura, S. (1995) *J. Am. Chem. Soc.*, **117**, 405–410.
- Kalbitzer, H.R., Gorler, A., Li, H., Dubovskii, P.V., Hengstenberg, W., Kowolik, C., Yamada, H. and Akasaka, K. (2000) *Protein Sci.*, **9**, 693–703.
- Koradi, R., Billeter, M. and Wüthrich, K. (1996) *J. Mol. Graphics*, **14**, 51–55.
- Kundrot, C.E. and Richards, F.M. (1987) *J. Mol. Biol.*, **193**, 157–170.
- Li, H., Yamada, H. and Akasaka, K. (1998) *Biochemistry*, **37**, 1167–1173.
- Li, H., Yamada, H. and Akasaka, K. (1999) *Biophys. J.*, **77**, 2801–2812.
- Lin, J., Westler, W.M., Cleland, W.W., Markley, J.L. and Frey, P.A. (1998) *Proc. Natl. Acad. Sci. USA*, **95**, 14664–14668.
- Linowski, J.W., Liu, N.-I. and Jonas, J. (1976) *J. Magn. Reson.*, **23**, 455–460.
- Linowski, J.W., Liu, N.-I. and Jonas, J. (1976) *J. Chem. Phys.*, **65**, 3383–3384.
- LiWang, A. C. and Bax, A. (1997) *J. Magn. Reson.*, **127**, 54–64.
- Pervushin, K., Ono, A., Fernandez, C., Szyperski, T., Kainosho, M. and Wüthrich, K. (1998) *Proc. Natl. Acad. Sci. USA*, **95**, 14147–14151.
- Pimentel, G.C. and McClellan, A.L. (1960) *The Hydrogen Bond*, Freeman & Co., San Francisco, CA.
- Sareth, S., Li, H., Yamada, H., Woodward, C.K. and Akasaka, K. (2000) *FEBS Lett.*, **470**, 11–14.
- Tjandra, N. and Bax, A. (1997) *J. Am. Chem. Soc.*, **119**, 8076–8082.
- Wagner, G. (1984) *Q. Rev. Biophys.*, **16**, 1–57.
- Wagner, G., Pardi, A. and Wüthrich, K. (1983) *J. Am. Chem. Soc.*, **105**, 5948–5949.
- Wang, Y.-X., Jacob, J., Cordier, F., Wingfield, P., Stahl, S.J., Huang, S. L., Torchia, D., Grzesiek, S. and Bax, A. (1999) *J. Biomol. NMR*, **14**, 181–184.
- Wishart, D.S., Bigam, C.G., Yao, J., Abildgaard, F., Dyson, H.J., Oldfield, E., Markley, J. L. and Sykes, B. D. (1995) *J. Biomol. NMR*, **6**, 135–140.
- Yamada, H. (1974) *Rev. Sci. Instrum.*, **45**, 640–642.